Received: 21 February 2022 | Revised: 3 April 2022 | Accepted: 5 April 2022

DOI: 10.1002/sia.7098

RESEARCH ARTICLE

SURFACE and INTERFACE ANALYSIS WILEY

Electron inelastic mean free path (IMFP) values of Kapton, polyethylene (PE), polymethylmethacrylate (PMMA), polystyrene (PS) and polytetrafluoroethylene (PTFE) measured with elastic peak electron spectroscopy (EPES)

Wolfgang S. M. Werner[1] | Fabian Helmberger[1] | Manuel Schürrer[1] | Olga Ridzel[2] | Michael Stöger-Pollach[3] | Christoph Eisenmenger-Sittner[3]

[1]Institut für Angewandte Physik, Vienna University of Technology, Vienna 1040, Austria

[2]Schlumberger Moscow Research Center, Moscow 125171, Russia

[3]Institut für Festkörperhysik, Vienna University of Technology, Vienna 1040, Austria

Correspondence
Wolfgang S.M. Werner, Institut für Angewandte Physik, Vienna University of Technology, Wiedner Hauptstrasse 8-10, A 1040 Vienna, Austria.
Email: werner@iap.tuwien.ac.at

Funding information
European Association of National Metrology Institutes, Grant/Award Number: 14IND12 EMPIR; FP7 Coordination of Non-Community Research Programmes, Grant/Award Number: PITN606988; FP7 People: Marie-Curie Actions Initial Training Network (ITN) SIMDALEE2, Grant/Award Number: PITN 606988

Elastic peak electron spectroscopy (EPES) was employed to measure the inelastic mean free path (IMFP) for energies between 500 and 1600 eV for five insulating organic compounds: Kapton, polyethylene (PE), poly(methyl methacrylate) (PMMA), polystyrene (PS) and polytetrafluoroethylene (PTFE). A Ni and a Si sample were used as reference materials to avoid measurement of the elastic reflection coefficient in absolute units. Correction of experimental elastic peak intensities for surface excitations was performed which turned out to be essential. The results are compared with recent evaluations of optical constants to yield the IMFP in the literature giving satisfactory agreement, with deviations generally below 20%. Investigation of the kinematics in an electron reflection experiment shows that the dispersion coefficient used in REELS data analysis cannot be identified with the true plasmon dispersion.

KEYWORDS
AES, elastic peak electron spectroscopy, inelastic mean free path, Kapton, organic polymers, plasmon dispersion, polyethylene, polymethylmetacrylate, polystyrene, polytetrafluoroethylene, XPS

1 | INTRODUCTION

X-ray Photoelectron Spectroscopy (XPS) is one of the most important surface analytical techniques in many fields of fundamental and applied science and technology.[1] In recent years, a surge in the interest in XPS applications in life sciences is evident in the literature.[2,3] Investigating the chemistry as well as quantification of shell thicknesses of core-shell nanoparticles with XPS will be of increasing importance since regulations of state institutions, such as the EU, will require corresponding information on consumer products in the near future.[4]

For quantification of XPS data as well as for calibration of nanoscale dimensions employing electron beam attenuation, it is imperative to have reliable values of the electron inelastic mean free path (IMFP) at one's disposal. The work by Shinotsuka, Tanuma, Powell and Penn[5–12] is the most important point of reference in this connection. These authors recently published a comprehensive report on IMFP values for 14 organic compounds (and water) in the energy range between 50 eV and 200 keV.[12] This was done by employing optical constants found in the literature,[13–17] and linear response theory was used to derive IMFP values. They compared their results with the so-called TPP-2M formula, developed by these authors, which allows a

quantitative estimate of IMFP values to be made for arbitrary materials and electron energies. An important conclusion of that paper was that the TPP-2M guideline accurately reproduces IMFP values for organic materials over the energy range studied by these authors.

Optical constants of several organic materials in the UV-range of energies have recently been measured by the group of the present authors[18] by means of reflection electron energy loss spectroscopy (REELS). For some of these materials, optical data were available in the literature, either measured by means of optical techniques,[19–22] with the transmission electron microscope[23] or by means of REELS.[24,25] The measurements based on electron scattering in a reflection geometry, REELS,[18,24,25] are clearly the most simple ones in terms of experimental effort, but suffer from the drawback that the recorded loss spectra constitute an average over all allowed momentum transfers in an inelastic collision. This implies knowledge of the plasmon dispersion relation used to extrapolate the zero momentum transfer data onto the complex plane.[18,24] The other methods mentioned above essentially sample the dielectric function at zero momentum transfer.[13,26] Satisfactory quantitative agreement with earlier results was found by Ridzel et al[18] for all materials for which literature data were available. As is commonly done for the interpretation of REELS spectra of insulators,[24,25] Ridzel et al[18] assumed that the energy loss features observed in REELS exhibit (almost) no dispersion.

When these optical constants are used to calculate IMFP values, almost perfect agreement is found with the data by Shinotsuka et al. when a quadratic dispersion is assumed. Quadratic dispersion implies that the resonance frequency ω_i of any given oscillator in the dielectric function changes with momentum transfer q according to

$$\omega_i(q) = \omega_i(q=0) + \alpha q^2/2, \quad (1)$$

with α being equal to unity. Note that atomic units are used above as well as below unless otherwise noted. However, setting $\alpha = 0$, dramatically lower values for the IMFP are obtained, as indicated by the blue dash-dotted curves in Figure 4.

This finding makes it clear that it is necessary to subject the Shinotsuka et al. data to an independent test without resorting in any way to using optical constants or linear response theory. This is the motivation for the present work in which the IMFP values of 5 insulating organic compounds (Kapton, polyethylene [PE], poly(methyl methacrylate) [PMMA], polystyrene [PS] and polytetrafluoroethylene [PTFE]) were measured using elastic peak electron spectroscopy (EPES) for energies between 500 and 1600 eV. Note that the EPES method relies on *elastic* electron scattering experiments merely using knowledge of the *elastic* scattering cross section to quantify IMFP values and does not need any elements of linear response theory or optical constants. Values for the elastic scattering cross section are readily available from e.g. the ELSEPA database.[27] The uncertainty in the elastic cross section is believed to be significantly smaller than the uncertainty in IMFP values, making EPES an attractive technique to verify or improve results for the IMFP.

Within the experimental error, we find rather excellent agreement for the IMFP values with the Shinotsuka et al. data when the present elastic peak intensities are corrected for surface excitations, as outlined by Werner et al.[28] This conclusion is obviously good news for quantification of arbitrary organic materials with XPS in chemistry or life sciences in that it (indirectly) implies that the TPP-2M formula provides a realistic guideline to predict IMFP values for arbitrary organic materials. On the other hand, our findings imply that the dispersion coefficient as used in the interpretation of REELS data is not related in a straightforward way to the actual dispersion of loss features in inelastic electron scattering. This is confirmed by a recent measurement of the plasmon dispersion of PMMA and PTFE in a transmission electron microscope (TEM)[29] and indicates that the kinematics in REELS experiments need further study.

2 | EXPERIMENTAL

The samples used in this study comprise Kapton, polyethylene (PE), poly(methyl methacrylate) (PMMA), polystyrene (PS) and polytetrafluoroethylene (PTFE). In addition, a piece of an *n*-doped silicon-wafer and a Ni-film sputtered on a Si-wafer were measured to avoid measurement in absolute units. While Ni has been proposed as a reference material,[32] we decided to to use an additional reference material (Si) to verify consistency and eliminate eventual systematic errors associated with the reference measurements. The method of sample preparation as well as further experimental details can be found in previous studies.[18,28] The REELS spectra were acquired under UHV conditions in a modified VG ESCALAB MkII spectrometer equipped with a hemispherical mirror analyser with five channeltrons operated at a pass energy of 20 eV. For each of the channeltrons, the deadtime was measured to be about 250 ns. A Kimball Physics ELG-2 electron gun was used as a primary electron source. The incident current of about 0.7 nA was measured for each spectrum with the Faraday cup built on to the electron source. Total countrates during the experiments were below 2×10^6 Hz. The angles of incidence and emission amounted to 60°, relative to the surface normal. The sample height was automatically adjusted for each sample to the optimal position by the stepper motor-controlled manipulator. The pressure in the analysis chamber during the measurement did not exceed 2×10^{-10} mbar. REELS spectra were measured for energies of 500, 700, 1000, 1200, 1500 and 1600 eV. Each spectrum was measured twice; the reported IMFP values are the average of both measurements. For mitigation of charging, the procedure described by Ridzel et al[18] was followed.

3 | DATA ANALYSIS

The elastic peak of the raw experimental spectra was fitted by a Gaussian, providing the peak area, as illustrated in Figure 1 for the spectra of Kapton. While the quality of the fit is generally good, a few data points near the peak maximum are not properly captured by a Gaussian peak shape (see, e.g., the data for 700 and 1000 eV in

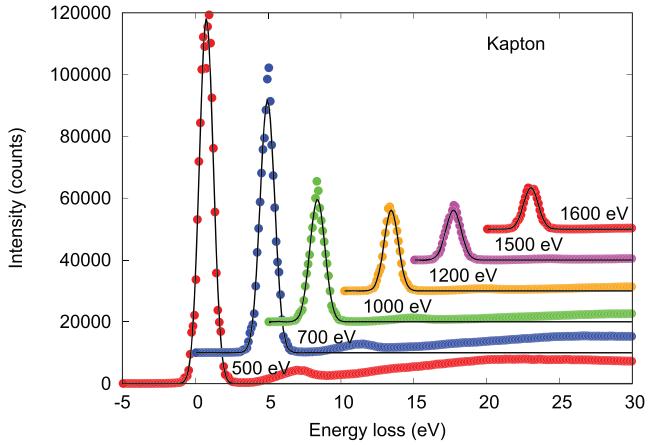

FIGURE 1 Elastic peak spectra of Kapton (data points) for the employed energies shown together with the fits to a Gaussian function (black curves) for the indicated energies

Figure 1). This is in contrast to elastic peak spectra of conductors, which, when recorded with our experiment, are found to be truly perfectly described by a Gaussian peak shape. This minor effect is attributable to differential charging limiting the accuracy of the measurement of the elastic peak intensity to about 10%, while for conductors it is of the order of 5% in our experiments.

When an electron coming from vacuum strikes the surface of a solid it may be deflected into the direction of the analyser by means of the Coulomb force of the atomic nuclei in the surface. Since this can occur at any depth after one or more elastic collisions with the ionic subsystem of the solid, it follows that the pathlength travelled inside the solid is not unique. Rather, the pathlengths s travelled by an ensemble of trajectories are described by the so-called pathlength distribution $Q(s)$. This quantity can be obtained for non-crystalline solids by solving a Boltzmann-type kinetic equation[30] and is fully described by the details of the *elastic* scattering process. No information whatsoever on the *inelastic* electron-solid interaction is required. This property makes the EPES technique uniquely useful for an independent verification of IMFP results derived from optical constants.

Since the inelastic mean free path, λ, is defined as "*the average distance an electron travels in between successive inelastic collisions (measured along the trajectory)*" and multiple inelastic scattering follows the Poisson stochastic process, the elastic peak intensity or zero-order partial intensity C_0, is related to the IMFP via[28,31,32]

$$C_0 = \int_0^\infty Q(s)\exp(-s/\lambda)ds. \tag{2}$$

The above equation explains the sensitivity of the zero-loss peak to the value of the IMFP: For small values of λ, the exponential function in Equation (2) is small and the probability for reflection without loss is expected to be small compared with the case where loss processes are more unlikely, that is, for large values of the IMFP.

According to the boundary conditions of Maxwell's equations, an electron may also experience an energy loss during the crossing of the vacuum-solid interface, either on the way in or on the way out of the surface.[33–35] Since the extent of the corresponding surface scattering zone $\langle z_{ss}\rangle$ is small compared with the mean distance between large angle collisions, λ_{tr}, the so-called elastic transport mean free path, $\langle z_{ss}\rangle \ll \lambda_{tr}$, it follows that the path within the surface scattering zone is approximately rectilinear.[36] The corresponding pathlength distribution then resembles a delta function $\delta(s-\langle z_{ss}\rangle)$, and according to Equation (2), an electron beam crossing the surface is attenuated by a factor[36]

$$\exp(-\mu_s), \tag{3}$$

where μ_s is the average number of surface excitations for a single surface crossing. In the present work, we use the formula proposed by Oswald to estimate μ_s[37,38]:

$$\mu_s = \frac{4}{a_s\sqrt{E}+2}. \tag{4}$$

where double surface crossing at 60° was accounted for. The values of the material parameter a_s are shown in Table 1 and were taken from Werner et al.[28]

Finally, accounting for the experimental sensitivity owing to the detector efficiency, solid angle and transmission function of the analyser, and so forth, by means of an energy dependent factor $T(E)$, the experimental elastic reflection coefficient $I_e(E)$ for a given primary current I_p hitting the surface is written as

$$I_e(E) = I_p T(E)\exp(-\mu_s)\int_0^\infty Q(s)\exp(-s/\lambda)ds. \tag{5}$$

Since we were unable to determine the experimental factor $T(E)$ with sufficient accuracy, we cannot use absolute elastic peak intensities to retrieve the IMFP. We therefore use reference materials for which the IMFP is assumed to be known. Denoting the reference materials and the investigated polymers by the subscript "r" and "x", respectively, we write for the ratio of elastic peaks, corrected for surface excitations:

$$\eta(\lambda_x) = \left(\frac{I_{e,x}/I_{p,x}}{\exp(-\mu_{s,x})}\right)\left(\frac{\exp(-\mu_{s,r})}{I_{e,r}/I_{p,r}}\right) = \frac{1}{C_{0,r}^{MC}}\int_0^\infty Q_x^{MC}(s)\exp(-s/\lambda_x)ds. \tag{6}$$

In the present work, the pathlength distributions $Q(s)$ were calculated by means of Monte Carlo (MC) simulations.[31,32,39–44] The only input parameter for this procedure is the differential cross section for elastic scattering which was obtained from the ELSEPA software.[27] The simulation algorithm starts with an electron at the surface travelling along the incident direction followed by a rectilinear segment. The length of this segment is established, as is commonly done in

TABLE 1 Values for the surface excitation parameter a_s[28] in units of $a_{NFE} = 0.173eV^{1/2}$ as well as retrieved values of the IMFP (in nm) for the Si and Ni reference (columns labelled "λ_{Si}" and "λ_{Ni}," respectively), for PS, PTFE, PMMA, Kapton and PE[28,38]

	PS ($a_s = 5.9$)			PTFE ($a_s = 3.6$)			PMMA ($a_s = 7.4$)			KAPT ($a_s = 12.2$)			PE ($a_s = 13.4$)			Si	Ni
E (keV)	λ_{Ni} (nm)	λ_{Si} (nm)	λ_{TP} (nm)	λ_{Ni} (nm)	λ_{Si} (nm)	λ_{TP} (nm)	λ_{Ni} (nm)	λ_{Si} (nm)	λ_{TP} (nm)	λ_{Ni} (nm)	λ_{Si} (nm)	λ_{TP} (nm)	λ_{Ni} (nm)	λ_{Si} (nm)	λ_{TP} (nm)	λ_{Ref} (nm)	λ_{Ref} (nm)
0.5	1.80	1.47	1.75	2.06	1.64	1.97	2.37	1.91	1.81	1.99	1.61	1.64	1.86	1.52	2.06	1.47	0.95
0.7	2.66	2.28	2.26	2.76	2.32	2.50	3.17	2.71	2.33	3.05	2.60	2.10	2.98	2.56	2.65	1.88	1.17
1.0	3.55	3.16	2.98	3.12	2.75	3.27	4.27	3.80	3.06	3.62	3.22	2.77	3.53	3.15	3.50	2.45	1.49
1.2	4.16	3.82	3.45	3.37	3.08	3.76	4.85	4.46	3.54	3.96	3.64	3.20	3.83	3.51	4.05	2.82	1.72
1.5	3.84	3.84	4.13	3.11	3.11	4.48	4.81	4.80	4.23	3.66	3.66	3.82	3.82	3.81	4.85	3.46	2.03
1.6	4.42	4.28	4.35	3.52	3.41	4.71	4.92	4.76	4.46	4.25	4.11	4.02	4.61	4.46	5.11	3.57	2.13

Note: The columns labelled "Si" and "Ni" show the IMFP values used for the reference materials which are presented in the last two columns labelled "λ_{ref}" and were taken from Shinotsuka et al.[9] The values given by the TPP-2M-formula are shown in the columns labelled "λ_{TP}." The surface excitation parameter for Si and Ni was $a_{s,Ni} = 1.7$ and $a_{s,Si} = 0.9$.

Monte Carlo calculations, by drawing a random sample from an exponential distribution with the elastic mean free path as characteristic length. The position as well as the pathlength travelled inside the solid is updated. Subsequently, a polar scattering angle is sampled from the differential elastic scattering cross section, and the direction of motion is updated, assuming azimuthal scattering angles to be uniformely distributed. The above steps are repeated until the particle exits the surface or its pathlength exceeds a given predefined limit. If the electron escapes from the surface with a direction outside the opening angle of the analyser or the particle remains inside the solid and its pathlength exceeds the chosen limit, the trajectory is discarded. Otherwise, the histogram of travelled pathlengths is updated. For the present work, 10^8 trajectories were simulated, resulting in a statistical error of the zero order partial intensity far below a percent. Note that the above algorithm does not use any information about inelastic scattering whatsoever. Inelastic scattering enters the picture retrospectively, via Equation (2).

Since the IMFP of the reference material is assumed to be known, a Monte Carlo (MC) simulation for Q_r^{MC} can be used to calculate the elastic reflection coefficient $C_{0,r}^{MC}$ via Equation (2). Subsequently, calibration curves relating the elastic peak intensity ratios to the IMFP values of the polymers as per Equation (6) were established for all energies and materials. These were fitted by a second order polynomial and used to retrieve the IMFP value corresponding to the measured intensity ratio.

A typical example is shown in Figure 2 for PS for 700 eV. The dependence of the intensity ratio is approximately linear, implying that the relative error in the resulting IMFP is equal to the relative error in the peak intensity ratio. The black dash-dotted arrow in Figure 2 shows the result when surface excitations are ignored ($\mu_s = 0$ in Equation 6), the red arrow gives the result when realistic values of μ_s are used which gives a result close to the one reported by Shinotsuka et al.[12]

A final aspect of the data analysis is the comparison between the MC elastic peak intensities (in absolute units) with the experimental

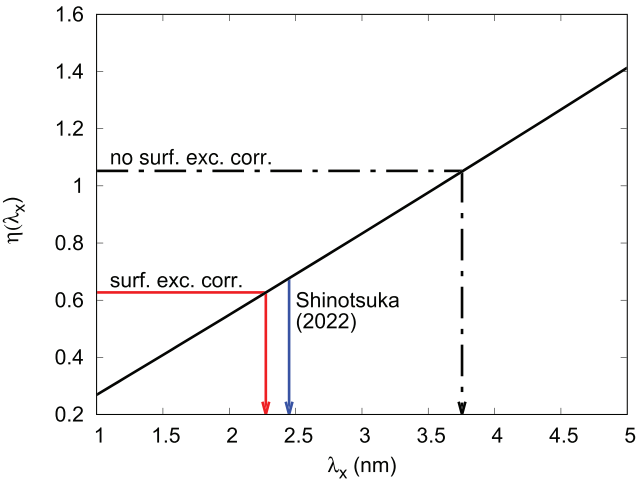

FIGURE 2 Illustration of the procedure to calibrate the IMFP using the Si reference for PS, for 700 eV. Black solid curve: polynomial fit of the result of the ratio $\eta(\lambda_x)$ of the reflection coefficient of the unknown and the reference sample calculated with the MC technique. Red arrow: experimental result after correction for surface excitations; black dash-dotted arrow: without surface excitation correction; the blue arrow indicates the IMFP value of Shinotsuka et al.[12]

results. According to Equation (5) this requires the energy dependence of the experimental sensitivity $T(E)$ to be calibrated, which is a difficult task. We circumvent this problem by normalising our data with the Si data by correcting the experimental peak intensities for surface excitations and dividing the Si data by the corresponding MC results. The resulting experimental sensitivity was satisfactorily described by a second degree polynomial $T(E) = a_2E^2 + a_1E + a_0$, with $a_2 = 8.4e-06, a_1 = -0.038$ and $a_0 = 51.96$. For the calculation of the MC peak intensities, we use Equation (2) in combination with the TPP-2 M formula[12] for the IMFP.

4 | RESULTS AND DISCUSSION

After correcting the experimental data for surface excitations and the experimental sensitivity, as explained in the previous paragraph, a comparison with the MC results for the zero order bulk partial intensities can be made in absolute units. This is illustrated in Figure 3 where the upper panel shows the normalised experimental results and the MC results using the TPP-2 M formula to estimate the IMFP are given in the lower panel. The typical error of about ~ 15% for the peak area ratio η is indicated in the experimental data for Ni.

Within the experimental uncertainty, a reasonable qualitative agreement is observed between experiment and the MC calculations. For the Si data, quantitative agreement is seen, as expected since the Si MC data were used to normalise the experimental intensities. For the other materials quantitative deviations are seen which is not surprising since it has to be kept in mind that the TPP-2 M formula was used for the IMFP values in Figure 3, which may be quantitatively different from the value of the IMFP consistent with our experimental peak intensities.

The IMFP values consistent with the experimental peak intensities are shown in Figure 4 and compared with literature data. When the experimental intensities are corrected for surface excitations, we obtain IMFP values represented by the filled red symbols when using the Ni reference, while the blue data points correspond to the

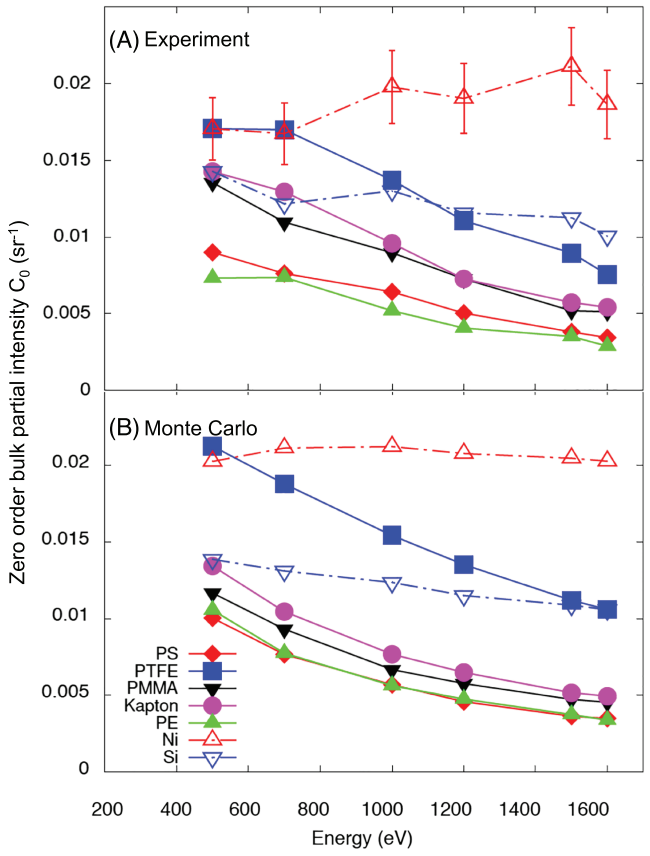

FIGURE 3 (A) Experimental data for the zero order bulk partial intensities (Equation 2) for the investigated materials (PS: red diamonds; PTFE: blue squares; PMMA: black downward triangles; Kapton: magenta circles; and PE; green upward triangles) as well as the employed reference materials (Ni: open red upward triangles; and Si: open blue downward triangles) for energies between 500 and 1600 eV. These data were obtained from the raw experimental peak intensities, normalised by the current during the measurement and corrected for surface excitations as well as the energy dependence of the experimental sensitivity (see text). (B) same as (A) but obtained from Monte Carlo calculations, as per Equation (2), that is, bulk zero order partial intensities C_0 (without accounting for surface excitations)

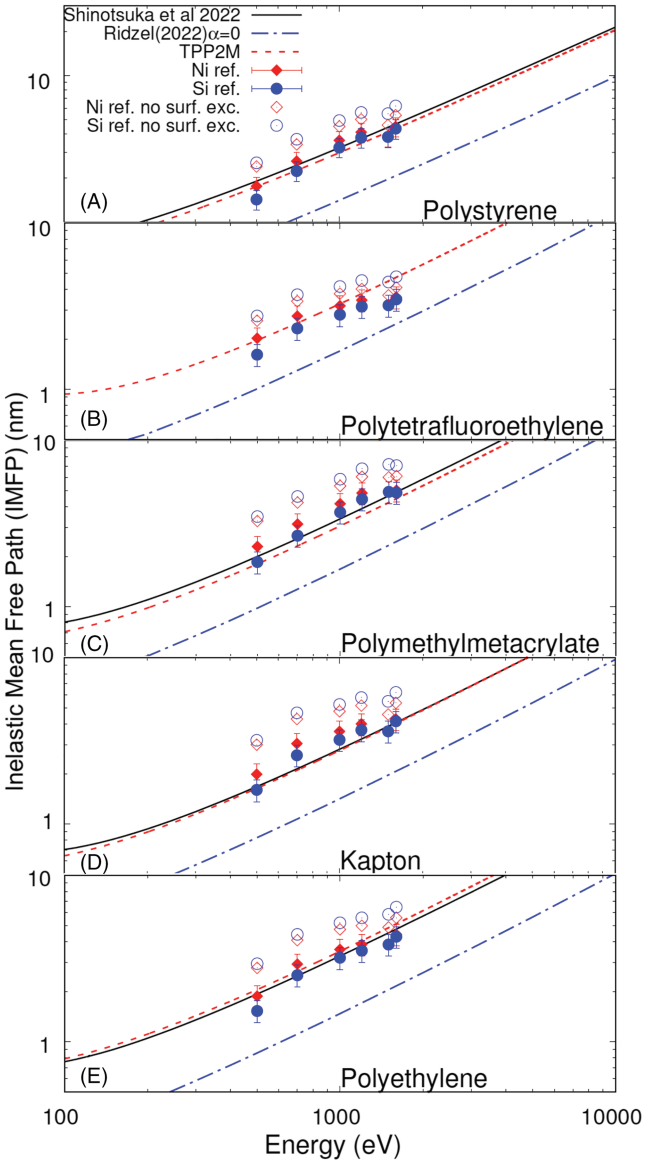

FIGURE 4 IMFP values derived from the present elastic peak measurements (datapoints) for the investigated materials: PS (A), PTFE (B), PMMA (C), Kapton (D) and PE (E). Open datapoints: without correction for surface excitations; filled datapoints: after correction for surface excitations; red datapoints: Ni reference; blue datapoints: Si reference; solid black curve: IMFP values from Shinotsuka et al.[12]; red dashed curve: TPP2M-formula[11]; blue dash-dotted curve: calculation of the IMFP using Equation (7) and optical constants from Ridzel et al[18] for zero dispersion ($\alpha = 0$ in Equation 1)

evaluation based on the Si reference. For comparison, open symbols show the results obtained when surface excitations are neglected. In this case, the retrieved IMFP values are consistently higher by almost a factor of two. This is not unexpected since the effect of surface excitations in polymers was recently found to be rather insignificant for the investigated polymers[28] while it was earlier shown to be appreciable for metals and nearly-free-electron materials.[38] The black curves represent the data for the IMFP reported by Shinotsuka et al., which are in very good agreement with the TPP-2M predictive formula, displayed as the red dashed curves.

In the non-relativistic range of energies, the IMFP can be calculated using[12]

$$\lambda(E)^{-1} = \frac{1}{\pi(E-E_g)} \int_{E_g}^{E-E_g-E_v} d\omega \int_{q_-}^{q_+} \frac{dq}{q} \mathrm{Im}\left[\frac{-1}{\epsilon(\omega,q)}\right]. \quad (7)$$

Here, the primary energy of the incoming electron is denoted by E and the energy loss function $\mathrm{Im}[-1/\varepsilon(\omega,q)]$ is expressed in terms of the dielectric function $\varepsilon(\omega,q)$, double differential with respect to the energy loss ω and the momentum transfer q. The limits of integration over the momentum transfer q depend on the incident energy E and the energy loss ω and are a consequence of energy and momentum conservation[31]:

$$q_\pm = \sqrt{2(E-E_g)} \pm \sqrt{2(E-E_g-\omega)} \quad (8)$$

In the above, E_g is the bandgap energy, and E_v is the width of the valence band for semiconductors and insulators.

Using Equations (7) and (8), IMFP values have also been calculated using the optical constants of Ridzel et al.[18] In doing so, perfect agreement is found (not shown) when evaluated using $\alpha = 1$ in the dispersion equation (1), while the blue dash-dotted curve, which represents the case $\alpha = 0$, yields IMFP values which are significantly smaller by a factor of 2–3 (!).

As stated above, by virtue of the linearity of the calibration curves such as the one shown in Figure 2, the relative experimental error in the IMFP values is equal to the relative uncertainty in the quantity η, leading to a typical error of about 15% in the retrieved IMFPs. Taking this into account the present data using Si as a reference material are seen to generally agree with the literature values within the statistical error. Comparison with Figure 3 also reveals that whenever the retrieved IMFP matches the TPP-2M value, the peak area ratios for the MC results and experiment are identical. A case in point is the result for Kapton, 500 eV, using the Si reference, where the TPP2 M and our IMFP results match perfectly and, in consequence, identical peak area ratios are seen in Figure 3. For PTFE, a rather significant deviation between the TPP-2M data and our results for the Si reference is seen, which can be also recognised in Figure 3.

However, there is a systematic inconsistency between the results for the two reference materials. Using Si as reference, the IMFP is always lower by 15–20% compared with the Ni-reference data. The reason for this systematic deviation is unclear at present, but might be due to sample preparation or, possibly, the values of the IMFP used for the reference materials. However, the validity of the IMFP values of the reference materials has been verified independently.[32,40,42]

Nonetheless, the general conclusion which can be drawn from Figure 4 is that the Shinotsuka et al. data[12] are confirmed by our present measurements in the investigated energy range. Note that this indirectly also implies a verification of the TPP-2M-formula which can be used for arbitrary polymers, as well as for any other material and energy.

The calculation of these authors relies on a quadratic dispersion of the energy loss function, through the use of the Penn algorithm, which is therefore also explicitly proven to be correct by our measurements, since our analysis is based on elastic peak data and we do not need to make any assumptions about the kinematics in an inelastic collision. The only aspect of inelastic scattering important to the present work is the stochastic process for multiple scattering (the Poisson process) which for non- crystalline solids, follows from the Boltzmann kinetic equation for electron transport.[45]

In contrast to this, the commonly employed method for the analysis of REELS spectra to obtain optical constants assumes that for insulators $\alpha = 0$,[18] or, alternatively, uses the dispersion constant α as a free parameter when fitting the model dielectric function to experimental spectra.[24] For insulators, this indeed yields values of α very close to zero,[24] consistent with the approach in Ridzel et al.[18] In the calculation of the IMFP, the choice of $\alpha = 0$ leads to an underestimation of the IMFP by a factor of two to three (as illustrated by the blue dash-dotted curves in Figure 4).

It is sometimes stated in the literature[46] that the value of the dispersion coefficient is related to the effective electron mass in the one-electron band structure of a solid, that is, the dispersion of the energy bands. Generally the REELS spectrum resembles the joint density of states, which represents all allowed electronic transitions accompanying a given energy loss. It is then tempting to assume that for an insulator with flat bands, vertical transitions ($q = 0$) will dominate while for metals, for which the conduction band minimum is often free-electron-like, a quadratic dispersion of the plasmon results. Then the REELS spectrum for insulators would correspond to the case $\alpha = 0$ and the choice of $\alpha = 0$ for insulators and $\alpha = 1$ for conductors seems justified.

However, the question how the dispersion of the (bulk) plasmon, essentially a many body-phenomenon, is related to the one-electron band structure, is by no means straightforward, in particular for insulators.[47–49] Furthermore, for large momentum transfers, the incoming electron essentially interacts with a single solid state electron near the so-called Bethe-ridge[50] in the electron-hole continuum. Then, the collision kinematics can be treated classically and a quadratic dispersion is a fundamental requirement dictated by energy conservation.

Plasmon dispersion is an essential phenomenon since a momentum dependent plasmon energy implies that the plasmon has a non-vanishing group velocity and, hence, can transport energy. For a jellium model, a quadratic plasmon dispersion follows from the linear

dependence of the electron gas pressure on the charge density.[49] Plasmon dispersion is not directly related to the electronic structure of the material, as long as the density of final states does not exhibit significant gaps.[51]

In a forthcoming publication, we have explicitly confirmed a quadratic plasmon dispersion for PMMA and PTFE[29] by measuring it in the TEM. This also follows indirectly from the consistency between the present IMFP values, which were determined from the decrease of the elastic peak in a reflection experiment due to inelastic scattering, and the IMFP values for the studied polymers, calculated by Shinotsuka et al,[12] on the basis of Penn's model, which implicitly assumes quadratic dispersion.

Summarising, we can state that it is not possible in a straightforward way to identify the dispersion constant α in Equation (1) used for interpretation of REELS spectra with the true plasmon dispersion. The question why the single scattering loss distribution in REELS behaves essentially different for conductors and polymers presently remains unresolved and should be addressed by future investigations to obtain a sound understanding of the kinematics relevant for inelastic scattering in REELS.

In this connection, the following observation might be useful: an essential difference exists between the inelastic collisions determining the intensity of the elastic peak and those inelastic processes responsible for the energy loss spectrum used in REELS analysis. The elastic peak intensity is decreased by inelastic scattering processes taking place at any depth a reflected electron may reach. The inelastic processes responsible for the intensity of the elastic peak are therefore representative for the bulk properties of the electron solid interaction. It then comes as little surprise that the present results based on elastic peak intensities, are consistent with the TEM results, since the latter obviously sample true bulk inelastic scattering processes. The same can be said for the consistency between the present EPES data and the IMFP values of Shinotsuka et al.

On the other hand, the loss spectrum used for REELS analysis is obtained after elimination of multiple scattering and is therefore representative for the group of electrons that have experienced a single inelastic collision. In consequence, the trajectories relevant for REELS are dominated by pathlengths of the order of the IMFP and the depth range where such inelastic collisions take place in a reflection geometry is equal to half the IMFP at most (for incidence and emission angles of 60° the relevant depth range is a quarter of the IMFP). Therefore, the single scattering distribution used for REELS analysis to extract optical constants is representative only for those inelastic scattering processes taking place in extreme proximity of the surface, while for the decrease of the elastic peak those inelastic processes are responsible which take place over a depth range spanning many IMFPs. In this sense, the elastic peak and the single scattering loss distribution are complementary.

The fact that in Werner et al[28] surface excitations were found to be very weak for insulators, in comparison with conductors, indicates that there is indeed a significant difference between conductors and insulators regarding the near surface electron-solid interaction. The physical reason why the surface polarisability of polymers on the one hand and conductors on the other hand behaves differently with regard to the scattering kinematics should be addressed from a theoretical point of view in a future investigation, a challenging task.[52]

5 | CONCLUSIONS

IMFP values for energies in the range between 500 and 1600 eV have been measured for five organic polymers using elastic peak electron spectroscopy. This technique relies exclusively on accurate knowledge of the elastic scattering cross section to retrieve the inelastic mean free path from elastic peak intensities. Taking into account the effect of surface excitations, we find rather good agreement with calculations of the IMFP by Shinotsuka et al,[12] derived from optical constants employing linear response theory and assuming a quadratic dispersion of the dielectric function. Measurements of the plasmon dispersion of PMMA and PTFE in the transmission electron microscope are consistent with this assumption.[29] On the other hand, for insulators, near-vertical transitions ($q \sim 0$) seem to dominate in the single scattering loss distribution extracted from reflection electron energy loss spectra to obtain optical constants. This would make plasmon dispersion irrelevant when interpreting the loss spectra, but it is unclear what causes the difference between conductors and insulators. While we do not have an explanation for this apparent contradiction, it can be concluded that care must be taken to interpret the dispersion coefficient α in reflection energy loss spectra as the true plasmon dispersion and the kinematics relevant for inelastic scattering in REELS needs further study.

ACKNOWLEDGEMENTS

The authors are grateful to Dr. M. Vos for fruitful discussions and wish to express their gratitude to Drs. C.J. Powell and S. Tanuma for helpful comments and suggestions as well as for sharing the data of Shinotsuka et al[12] before publication. Financial support by the 14IND12 EMPIR project InNanoPart within the European Union's Horizon 2020 research and innovation programme and by the FP7 People: Marie-Curie Actions Initial Training Network (ITN) SIMDALEE2 (Grant No. PITN 606988) is gratefully acknowledged. The computational results presented have been achieved using the Vienna Scientific Cluster (VSC). The authors acknowledge TU Wien Bibliothek for financial support through its Open Access Funding Programme.

DATA AVAILABILITY STATEMENT

Data will be made available upon reasonable request.

ORCID

Wolfgang S. M. Werner https://orcid.org/0000-0002-4870-9137
Fabian Helmberger https://orcid.org/0000-0002-9206-1315
Manuel Schürrer https://orcid.org/0000-0001-9587-1658
Olga Ridzel https://orcid.org/0000-0002-9972-3924
Michael Stöger-Pollach https://orcid.org/0000-0002-5450-4621
Christoph Eisenmenger-Sittner https://orcid.org/0000-0002-7096-6092

REFERENCES

1. Briggs D, Seah MP. *Practical Surface Analysis*. Chichester: Wiley; 1983.
2. Briggs D, Grant J. *Surface Analysis by Auger and X-Ray Photoelectron Spectroscopy*. Chichester UK: IM Publications; 2003.
3. Engelhard MH, Droubay TC, Du Y. *X-Ray Photoelectron Spectroscopy Applications*. Amsterdam: Elsevier; 2017;716-724.
4. Innanopart Euramet EMPIR Project. https://empir.npl.co.uk/innanopart/
5. Tanuma S, Powell CJ, Penn DR. Calculations of electron mean free paths for 31 materials. *Surf Interface Anal*. 1988;11:577.
6. Tanuma S, Powell CJ, Penn DR. Calculations of electron inelastic mean free paths. II. Data for 27 elements over the 50–2000 eV range. *Surf Interface Anal*. 1991;17:911-926.
7. Tanuma S, Powell CJ, Penn DR. Calculations of electron inelastic mean free paths (IMFPS). IV. Evaluation of calculated IMFPs and of the predictive IMFP formula TPP-2 for electron energies between 50 and 2000 eV. *Surf Interface Anal*. 1993;20:77-89.
8. Tanuma S, Powell CJ, Penn DR. Calculations of electron inelastic mean free paths. V. Data for 14 organic compounds over the 50–2000 eV range. *Surf Interface Anal*. 1994;21:165-176.
9. Shinotsuka H, Tanuma S, Powell CJ, Penn DR. Calculations of electron inelastic mean free paths. X. Data for 41 elemental solids over the 50 eV to 200 keV range with the relativistic full Penn algorithm. *Surf Interface Anal*. 2015;47:871-888.
10. Shinotsuka H, Da B, Tanuma S, Yoshikawa H, Powell CJ, Penn DR. Calculations of electron inelastic mean free paths. XI. Data for liquid water for energies from 50 eV to 30 keV. *Surf Interface Anal*. 2017;49:238-252.
11. Shinotsuka H, Tanuma S, Powell CJ, Penn DR. Calculations of electron inelastic mean free paths. XII. Data for 42 inorganic compounds over the 50 eV to 200 keV range with the full Penn algorithm. *Surf Interface Anal*. 2019;51:427-457.
12. Shinotsuka H, Tanuma S, Powell CJ. Calculations of electron in elastic mean free paths. XIII. Data for 14 organic compounds and water over the 50eV to 200keV range with the relativistic full Pennalgorithm. *Surf Interface Anal*. 2022;49:238. doi:10.1002/sia.7064
13. Palik ED. *Handbook of Optical Constants of Solids*. New York: Academic Press; 1985.
14. Palik ED. *Handbook of Optical Constants of Solids II*. New York: Academic Press; 1991.
15. Palik ED. *Handbook of Optical Constants of Solids I& II*. New York: Academic Press; 1991;1985.
16. Henke BL, Gullikson EM, Davis JC. X-ray interactions: photoabsorption, scattering, transmission, and reflection at E=50-30000 eV, Z=1-92. *At Data Nucl Data Tables*. 1993;54(2):181.
17. Cullen DE, Hubbell JH, Kissel L. EPDL97, The Evaluated Data Library. *tech rep*. 5. 1997 Version, UCRL-50400.
18. Ridzel OY, Kalbe H, Astašauskas V, Kuksa P, Bellissimo A, Werner WSM. Optical constants of organic insulators in the UV-range extracted from reflection electron energy loss spectra. *Surf Interface Anal*. 2022;54:487-500. doi:10.1002/sia.7055
19. Inagaki T, Hamm RN, Arakawa ET, Painter LR. Optical and dielectric properties of DNA in the extreme ultraviolet. *J Chem Phys*. 1974;61(10):4246-4250. doi:10.1063/1.1681724
20. Inagaki T, Arakawa ET, Hamm RN, Williams MW. Optical properties of polystyrene from the near-infrared to the x-ray region and convergence of optical sum rules. *Phys Rev B*. 1977;15(6):3243-3253. doi:10.1103/PhysRevB.15.3243
21. Arakawa ET, Williams MW, Ashley JC, Painter LR. The optical properties of Kapton: Measurement and applications. *J Appl Phys*. 1981;52(5):3579-3582. doi:10.1063/1.329140
22. Painter LR, Arakawa ET, Williams MW, Ashley JC. Optical Properties of Polyethylene: Measurement and Applications. *Radiat Res*. 1980;83(1):1. doi:10.2307/3575254
23. Ritsko JJ, Brillson LJ, Bigelow RW, Fabish TJ. Electron energy loss spectroscopy and the optical properties of polymethylmethacrylate from 1 to 300 eV. *J Chem Phys*. 1978;69(9):3931-3939. doi:10.1063/1.437131
24. Tahir D, Tougaard S. Electronic and optical properties of selected polymers studied by reflection electron energy loss spectroscopy. *J Appl Phys*. 2012;111(5):54101. doi:10.1063/1.3688327
25. Mondio G, Neri F, Patanè S, Arena A, Marletta G, Iacona F. Optical properties from reflection electron energy loss spectroscopy. *Thin Solid Films*. 1992;207(1-2):313-318. doi:10.1016/0040-6090(92)90143-Y
26. Egerton RF. *Electron Energy Loss Spectroscopy in the Electron Microscope*. New York and London: Plenum; 1985.
27. Salvat F, Jablonski A, Powell CJ. ELSEPA - Dirac partial-wave calculation of elastic scattering of electrons and positrons by atoms, positive ions and molecules. *Comp Phys Com*. 2005;165:157-190.
28. Werner WSM, Helmberger F, Schürrer M, Eisenmenger-Sittner C, Ridzel OY. Measurement of the surface excitation parameter of selected organic polymers. *Surf Interface Anal*. 2022. doi:10.1002/sia.7080
29. Werner WSM, Stöger-Pollach M, Ridzel OY. Measurement of the plasmon dispersion of PMMA and PTFE; 2022.
30. Werner WSM, Tilinin IS, Hayek M. Angular distribution of electrons reflected elastically from noncrystalline solid surfaces. *Phys Rev*. 1994;B50:4819.
31. Werner WSM. Electron transport in solids for quantitative surface analysis. *Surf Interface Anal*. 2001;31:141.
32. Powell CJ. Jabłonski A., Evaluation of calculated and measured electron inelastic mean free paths near solid surfaces. *J Phys Chem Ref Data*. 1999;28:19.
33. Ritchie RH. Plasma losses by fast electrons in thin films. *Phys Rev*. 1957;106:874.
34. Salvat-Pujol F, Werner WSM. Surface excitations in electron spectroscopy. Part I: dielectric formalism and Monte Carlo algorithm. *Surf Interface Anal*. 2013;45:873-894.
35. Salvat-Pujol F. Secondary-electron emission from solids Coincidence experiments and dielectric formalism. *PhD thesis*. Vienna: Vienna University of Technology; 2012.
36. Werner WSM. Obtaining Quantitative information on surface excitations from REELS. *Surf Interface Anal*. 2003;35:347.
37. Oswald R. Numerische Untersuchung der elastischen Streuung von Elektronen an Atomen und ihrer Rückstreuung an Oberflächen amorpher Substanzen im Energiebereich unter 2000 eV. *PhD thesis*. Tübingen: Eberhard-Karls-Universität Tübingen; 1992.
38. Werner WSM, Smekal W, Tomastik C, Störi H. Surface excitation probability of medium energy electrons in metals and semiconductors. *Surf Sci*. 2001;486:L461-6.
39. Zemek J, Jiricek P, Werner WSM, Lesiak B, Jablonski A. Angular-resolved elastic peak electron spectroscopy: experiment and Monte Carlo calculations. *Surf Interface Anal*. 2006;38:615-619.
40. Werner WSM, Tomastik C, Cabela T, Richter G, Störi H. Elastic electron reflection for determination of the inelastic mean free path of medium energy electrons in 24 elemental solids for energies between 50 and 3400 eV. *J Electron Spectrosc Rel Phen*. 2001;113:127.
41. Werner WSM, Tomastik C, Cabela T, Richter G, Störi H. Electron inelastic mean free path measured by elastic peak electron spectroscopy for 24 solids between 50 and 3400 eV. *Surf Sci*. 2001;470:L123.
42. Beilschmidt H, Tilinin IS, Werner WSM. Inelastic mean free path of medium energy electrons in Au, Pt, Ni and Al determined by elastic peak electron spectroscopy. *Surf Interface Anal*. 1994;22:120.
43. Werner WSM. Trajectory reversal approach for electron backscattering from solid surfaces. *Phys Rev B*. 2005;71:115415.
44. Dubus A, Jabłonski A. Tougaard, S. Prog Surf Sci; 2000.
45. Werner WSM. Slowing down of medium energy electrons in solids. *Phys Rev*. 1997;B55:14925.

46. Hajati S, Romanyuk O, Zemek J, Tougaard S. Validity of Yubero-Tougaard theory to quantitatively determine the dielectric properties of surface nanofilms. *Phys Rev*. 2008;B77:155403.
47. Ferrell RA, Quinn J. Characteristic energy loss of electrons passing through metal foils: momentum-exciton model of plasma oscillations. *Phys Rev*. 1957;108:570-575.
48. Horie C. Exciton and plasmon in insulating crystals. *Prog TheoPhys*. 1959;21:113-134.
49. Schattschneider P. *Fundamentals of Inelastic Electron Scattering*. New York, Vienna: Springer; 1986.
50. Vos M. A model dielectric function for low and very high momentum transfer. Nuclear Instruments and Methods in Physics Research. *Section B: Beam Interact Mater Atoms*. 2016;366:6-12. doi:10.1016/j.nimb.2015.09.091
51. Werner WSM, Asta-Csauskas V, Ziegler P, et al. Secondary electron emission by plasmon induced symmetry breaking in highly oriented pyrolitic graphite (HOPG). *Phys Rev Lett*; 2020:196603. doi:10.1103/PhysRevLett.125.196603
52. Feibelmann PJ. Surface electromagnetic fields. *Prog Surf Sci*. 1982;12:207-408.

How to cite this article: Werner WSM, Helmberger F, Schürrer M, Ridzel O, Stöger-Pollach M, Eisenmenger-Sittner C. Electron inelastic mean free path (IMFP) values of Kapton, polyethylene (PE), polymethylmethacrylate (PMMA), polystyrene (PS) and polytetrafluoroethylene (PTFE) measured with elastic peak electron spectroscopy (EPES). *Surf Interface Anal*. 2022;54(8):855-863. doi:10.1002/sia.7098